

REPORT DOCUMENTATION PAGE				Form Approved OMB No. 0704-0188	
<small>The public reporting burden for this collection of information is estimated to average 1 hour per response, including the time for reviewing instructions, searching existing data sources, gathering and maintaining the data needed, and completing and reviewing the collection of information. Send comments regarding this burden estimate or any other aspect of this collection of information, including suggestions for reducing the burden, to the Department of Defense, Executive Services and Communications Directorate (0704-0188). Respondents should be aware that notwithstanding any other provision of law, no person shall be subject to any penalty for failing to comply with a collection of information if it does not display a currently valid OMB control number.</small>					
PLEASE DO NOT RETURN YOUR FORM TO THE ABOVE ORGANIZATION.					
1. REPORT DATE (DD-MM-YYYY)		2. REPORT TYPE FINAL REPORT		3. DATES COVERED (From - To) 30 Sep 2005 - 30 Sep 2006	
4. TITLE AND SUBTITLE (DARPA) TOWARDS ON-CHIP ATOM TRANSITIONS			5a. CONTRACT NUMBER		
			5b. GRANT NUMBER FA9550-04-1-0460		
			5c. PROGRAM ELEMENT NUMBER 62712E		
			5d. PROJECT NUMBER T139/00		
6. AUTHOR(S) PROFESSOR ANDERSON			5e. TASK NUMBER		
			5f. WORK UNIT NUMBER		
7. PERFORMING ORGANIZATION NAME(S) AND ADDRESS(ES) UNIVERSITY OF COLORADO 3100 MARINE STREET BOULDER CO 80309-0572				8. PERFORMING ORGANIZATION REPORT NUMBER	
9. SPONSORING/MONITORING AGENCY NAME(S) AND ADDRESS(ES) AF OFFICE OF SCIENTIFIC RESEARCH 875 NORTH RANDOLPH STREET ROOM 3112 ARLINGTON VA 22203 DR ANNE MATSUURA				10. SPONSOR/MONITOR'S ACRONYM(S)	
				11. SPONSOR/MONITOR'S REPORT NUMBER(S)	
12. DISTRIBUTION/AVAILABILITY STATEMENT DISTRIBUTION STATEMENT A: UNLIMITED					
13. SUPPLEMENTARY NOTES					
14. ABSTRACT Atomtronics focuses on atom analogs of electronic materials, devices and circuits. A strongly interacting ultracold Bose gas in a lattice potential is analogous to electrons in solid-state crystalline media. As a consequence of the band structure, cold atoms in a lattice can exhibit insulator or conductor properties. P-type and N-type material analogs can be created by introducing impurity sites into the lattice. Current through an atomtronic wire is generated by connecting the wire to an atomtronic battery which maintains the two contacts at different chemical potentials. The design of an atomtronic diode with a strongly asymmetric current-voltage curve exploits the existence of superfluid and insulating regimes in the phase diagram. "The atomtronic analog of a bipolar junction transistor exhibits large negative gain". Our results provide the building blocks for more advanced atomtronic devices and circuits such as amplifiers, oscillators and fundamental logic gates.					
15. SUBJECT TERMS					
16. SECURITY CLASSIFICATION OF:			17. LIMITATION OF ABSTRACT	18. NUMBER OF PAGES	19a. NAME OF RESPONSIBLE PERSON
a. REPORT	b. ABSTRACT	c. THIS PAGE			19b. TELEPHONE NUMBER (Include area code)

20070516078

Atomtronics: ultracold atom analogs of electronic devices

B. T. Seaman, M. Krämer, D. Z. Anderson and M. J. Holland
JILA, National Institute of Standards and Technology and Department of Physics,
University of Colorado, Boulder CO 80309-0440, USA
(Dated: June 23, 2006)

Atomtronics focuses on atom analogs of electronic materials, devices and circuits. A strongly interacting ultracold Bose gas in a lattice potential is analogous to electrons in solid-state crystalline media. As a consequence of the band structure, cold atoms in a lattice can exhibit insulator or conductor properties. P-type and N-type material analogs can be created by introducing impurity sites into the lattice. Current through an atomtronic wire is generated by connecting the wire to an atomtronic battery which maintains the two contacts at different chemical potentials. The design of an atomtronic diode with a strongly asymmetric current-voltage curve exploits the existence of superfluid and insulating regimes in the phase diagram. The atomtronic analog of a bipolar junction transistor exhibits large negative gain. Our results provide the building blocks for more advanced atomtronic devices and circuits such as amplifiers, oscillators and fundamental logic gates.

I. INTRODUCTION

A collection of ultracold atoms subject to a spatially periodic potential can exhibit behavior analogous to electrons in a crystal lattice. This fact has been established in an impressive series of experiments with Bose-Einstein condensates and Fermi gases in optical lattices, that is, periodic potentials produced by interfering laser beams [1–10]. The analogy between ultracold atoms in lattice potentials and electrons in crystals is manifestly a rich one. It extends to strongly interacting ultracold Bose gases which exhibit both superfluid and insulating behavior and feature a gapped energy spectrum. The tunability of interactions in optical lattices has led to the spectacular demonstration of these properties [11, 12]. In this work we introduce analogs of electronic materials, including metals, insulators, and semiconductors, in the context of ultracold strongly interacting bosons. We use lattice defects to achieve behavior similar to doped P-type and N-type semiconductors. The interest is to adjoin P-type and N-type lattices to create diodes and then NPN or PNP structures to achieve behavior similar to that of bipolar junction transistors. We show that such heterogeneous structures can indeed be made to mimic their electronic counterparts. Ruschhaupt and Muga [13] have described an atom device with diode-like behavior, and Micheli et. al. [14] have proposed a single-atom transistor that serves as a switch (see also [15–19]). Both of these devices depend on control and coherence at the single atom level. Moreover, Stickney et. al. [20] have recently demonstrated that a Bose-Einstein condensate in a triple well potential can exhibit behavior similar to that of a field effect transistor. Our intent is to establish ultracold atom analogs of electronic materials and semiconductor devices that can be used to leverage the vast body of electronic knowledge and heuristic methods. From semiconductor materials, the analogy expands into what can be referred to as *atomtronics*. With diodes and transistors in hand, it is straightforward to conceive of atom amplifiers, oscillators, flip-flops, logic gates, and a host of other atomtronic circuit analogs to electronic cir-

cuits. Such a set of devices can serve as a toolbox for implementing and managing integrated circuits containing atom optical elements [21–23] or quantum computation components [24–26] and might be of particular interest in the context of rapidly advancing atom chip technologies [27, 28].

Atoms in periodic potential structures and electrons in solid state crystals have much in common. In both systems, particle motion occurs by tunneling through the potential barrier separating two lattice sites. A particle can delocalize over the entire lattice and sustain currents. Therefore, in atomtronic devices the dual of electric current is atomic flux. In both systems, currents are created when there is a potential gradient which causes the particles to move from a region of high potential to a region of low potential. In electronics, potentials arise from electrical fields. In atomtronics, potential gradients are understood in terms of chemical potentials. The characteristics of both electronic and atomtronic devices can be examined by using a battery to apply a potential difference across the system and observing the response in the current.

Different types of electronic conductors exist because electrons in a crystal structure occupy states of an energy spectrum that features a band structure. The materials can carry a current only if the highest occupied energy band is only partially filled with electrons. Under this condition, the system is a conductor. On the other hand, the system is an insulator if all occupied bands are full. The highest fully occupied band is called the valence band, while the lowest empty or partially occupied band is referred to as the conduction band.

Ultracold strongly interacting bosonic atoms in periodic structures behave similarly to their electronic counterparts. Strong repulsive interactions prevent atoms from occupying the same lattice site, mimicking the fermionic behavior of electrons. Hence, a current can flow easily as long as there are empty sites available. However, once the filling reaches one atom per site, the system becomes an insulator. A large energy gap given by the repulsive onsite interaction must be overcome in order

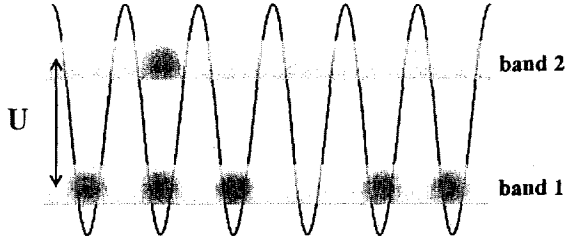


FIG. 1: Schematic of the atomtronic energy band structure of strongly interacting bosons in a lattice. The first band is made up of all states with a filling of less than one atom per site while the second band contains all states with filling between one and two atoms per site. The two bands are separated by the onsite interaction U .

to add another particle to this configuration. A particle added in excess of a filling of one atom per site can again carry a current since it can move around freely above the filled valence band of one atom per site. The system remains a conductor until it arrives at a filling of two atoms per site and it becomes an insulator again. Hence, as in electronics, there is a band structure and it is the filling of the bands which determines whether a material is a conductor or an insulator. The energy band structure of atoms in a lattice is depicted schematically in Fig. 1. The lowest band is made up of states having between zero and one atom per site. The next band contains all states with one to two atoms per site. This second band is separated from the first by a large energy gap on the order of the onsite repulsion. Higher bands are formed analogously. The highest occupied band of a conductor is only partially filled while insulators are characterized by full bands.

There are two major differences between usual electronic materials and the atomtronic materials considered here. First, the energy gap is due to the Pauli exclusion principle in the case of electrons while in the bosonic case the gap is due to the repulsive interaction between atoms. Second, the atomtronic conductor features superfluid rather than normal flow and in that sense resembles an electronic superconductor.

The purpose of this paper is to study the behavior of atomtronic materials in simple circuits and to show how to use these materials to build more complex circuit devices, namely diodes and bipolar junction transistors. The paper is structured as follows. Section II introduces the Bose-Hubbard formalism that will be used to describe the atomtronic systems. In particular, it discusses the zero temperature phase diagram, the properties of an atomtronic battery and the method we use to calculate current response to a voltage. Doped atomtronic materials and the current-voltage behavior of atomtronic wires will be discussed in Sec. III. A diode obtained by combining a P-type and N-type atomtronic material with a voltage bias applied by a battery is examined in Sec. IV. Section V presents the atom analog of a semi-

conductor bipolar junction transistor. Finally, Sec. VI contains remarks on possible applications, on the differences between our atomtronic devices and their electronic counterparts and on future perspectives.

II. BOSE-HUBBARD FORMALISM

The different kinds of atomtronic materials are best understood by examining the different zero temperature quantum phases of the system. We model the system of bosons in a 1D chain of lattice sites with the Bose-Hubbard Hamiltonian

$$\hat{H} = \frac{U}{2} \sum_i \hat{n}_i(\hat{n}_i - 1) - J \sum_{\langle ij \rangle} \hat{a}_i^\dagger \hat{a}_j + \sum_i (\epsilon_i - \mu) \hat{n}_i, \quad (1)$$

where \hat{a}_i is the annihilation operator for a particle at site i , $\hat{n}_i \equiv \hat{a}_i^\dagger \hat{a}_i$ is the number operator at site i , U is the onsite repulsive interaction strength, J is the hopping matrix element between nearest neighbors, $\langle ij \rangle$ labels nearest neighbors, ϵ_i is the external potential at site i and μ is the chemical potential of the system. The Bose-Hubbard Hamiltonian is obtained by retaining only the contributions of the lowest single particle Bloch band to the Hilbert space and by making a tight binding approximation (for a review see [29]). It yields an accurate description of an ultracold dilute Bose gas in a periodic potential. The zero temperature phase diagram of this Hamiltonian was first studied in [30].

For very large onsite repulsion, $U \gg J$, the system enters the regime of *fermionization* where bosons are impenetrable and only two Fock states, $|n_i\rangle$ and $|n_i + 1\rangle$, are needed at each site to accurately describe the system (two-state approximation). Note that this is equivalent to mapping bosonic operators onto fermionic ones via the Jordan-Wigner transformation [31, 32]. The data presented in this paper is obtained by considering the system described by the Hamiltonian Eq. (1) in the fermionized regime. We have verified that the error resulting from the two-state approximation becomes negligible for $U/J \geq 100$ (see also [33]).

A. Phase Diagram

The phase diagram of the Bose-Hubbard Hamiltonian contains the complete information about the band structure of the system for a given J/U , see Fig. 2 in which the phase diagram was created using the two-state approximation. At $T = 0$, the Bose-Hubbard model has two distinct phases, a Mott-insulating and a superfluid phase. The Mott-insulating phase is entered below a critical value of J/U for an integer number of particles per site. In this phase strong interactions completely block particle motion rendering the gas incompressible, that is $\partial n / \partial \mu = 0$, where n is the average filling of a site. The superfluid phase is obtained for non-integer filling.

Figure 2 presents the boundary between the conducting and insulating phases as a function of J/U and chemical potential μ/U . The two lobes limit the Mott-insulator zones with one atom per site (lower lobe, MI:1) and two atoms per site (upper lobe, MI:2). Insulator phases with higher integer filling are obtained at larger values of μ/U . The remainder of the phase diagram is in the conducting superfluid phase, labeled *SF*. No insulating phase exists for values of J/U larger than ~ 1 . Note that the triangular, non-rounded, shape of the Mott lobes in Fig. 2 is due to the two-state approximation becoming increasingly inaccurate as J/U is increased [34].

Each value of μ/U and J/U maps onto a particular lattice filling. In the fermionization regime ($J/U \ll 1$), an analytic expression for the relation between these parameters in the limit of a large number of lattices sites can be derived. It reads [35]

$$\mu = U(m - 1) + (-1)^m 2mJ \cos(\pi n), \quad (2)$$

where $m = 1, 2, \dots$ is the band index. Plotting the phase diagram as a function of μ/U rather than the number of particles is useful because then one can directly read out the band widths and the band gaps for a given J/U . As illustrated in Fig. (2), the width of the second band is given by the height of the second superfluid phase region at fixed J/U while the size of the band gap between first and second band is given by the height of the lowest insulating zone at that J/U . Hence, the details of the atomic band structure, such as the exact size of the band gap and height of a band, depend on the ratio J/U . In order to have access to both insulating and conducting phases, the ratio J/U must be small. If this ratio is too big there is no well defined band gap and therefore no transition to an insulating phase for integer filling. The basic ideas presented in this paper rely on this condition being satisfied. They do not require the stronger condition $J \ll U$ for fermionization. The latter condition is merely assumed to facilitate calculations.

B. Atomtronic Battery

Just as for electronic circuits, the atomtronic version of a battery is crucial but it is also subtle. In the following, we identify the basic properties and actions of the atomtronic analog of battery.

Energy for electronic circuits is supplied by sources of electric potential. Furthermore, electric potentials are used to set the bias points of circuit elements to achieve their desired behavior. For simplicity, we will use the term battery to refer to a device that provides a fixed potential difference and can supply an electric current or atom flux.

The voltage of a battery is fixed by the potential difference between two terminals. A specific potential difference between two points within a device or circuit is achieved by connecting those two points with the two battery terminals, or poles. In the electronic case the

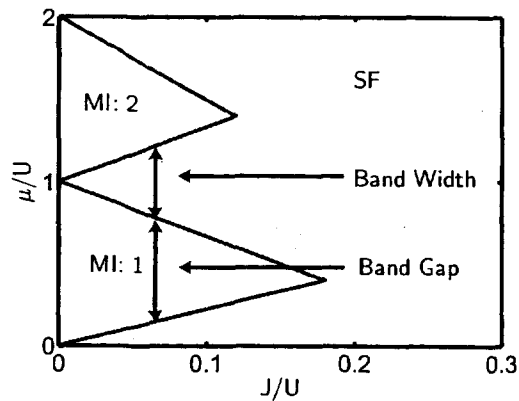


FIG. 2: Zero temperature phase diagram of a Bose gas obtained for a one-dimensional lattice using the two-state approximation. At large values of J/U the gas is superfluid (*SF*). Below a critical value of J/U the system enters a Mott-insulator phase (*MI*) for integer filling, while it remains superfluid for non-integer filling. The *MI* : 1 Mott-insulator region has one atom per site and the *MI* : 2 region has two atoms per site. The Mott lobe boundaries are not rounded due to the use of the two-state approximation [34].

value of electric potential at any one point in a circuit is arbitrary, as one is interested only in electric potential differences, in other words the voltage between two points. In the atomtronic case, the function of the battery is to hold the two contacts at two different values of the chemical potential, say μ_L on the left and μ_R on the right. The applied voltage is then defined by

$$V \equiv \mu_L - \mu_R. \quad (3)$$

The current flows from higher to lower chemical potential, i.e. from higher to lower voltage. Chemical potential difference in atomtronic system is analogous to electric potential difference in electronic systems.

To understand the physics underlying this concept, note that bringing the system in contact with a battery pole of chemical potential $\mu_L > \mu$ leads to the injection of Δn particles, where μ is the chemical potential of the isolated system. The magnitude of Δn is given by the difference in filling of states with chemical potential μ and μ_L . This information is contained in the phase diagram. The particle transfer increases with increasing μ_L within a superfluid region and becomes constant as μ_L is moved into a Mott insulating zone. In the fermionization regime, the magnitude of Δn is fixed by Eq. (2). The analogous reasoning applies to the removal of particles at the battery pole with $\mu_R < \mu$.

Feeding atoms into a circuit element through a contact at one end and removing them through a contact at the other end generates a current. Particles move from a region of excess to a region of deficit. This current reaches a steady state if the carrier excess at one end is replenished through one contact with the battery at the same

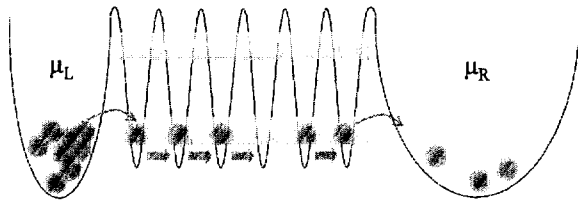


FIG. 3: Schematic of atoms in a lattice connected to an atomtronic battery. A voltage is applied by connecting the system to two reservoirs, one of higher (left) and one of lower chemical potential (right). An excess (deficit) of atoms is generated in the left (right) part of the system respectively giving rise to a current from left to right.

rate at which the deficit is maintained at the other end through the contact with the other pole of the battery.

Experimentally, a battery can be created by establishing two separate large systems which act as reservoirs each with its own constant chemical potential. These may also be lattice configurations or other experimentally plausible systems such as large harmonic traps containing a large number of atoms. Each of these reservoirs can be connected to one end of the atomtronic system and current is then possible from the higher chemical potential system to the lower one. This configuration is displayed in Fig. 3. From a practical point of view, the chemical potentials of the battery poles can be maintained by transferring atoms, possibly classically, between the two poles.

C. Computation of Current Response

To power a circuit, we connect the system to an atomtronic battery by bringing two reservoirs of different chemical potential μ_L and μ_R into contact with the two ends of the lattice. The values of μ_L and μ_R determine the particle transfer Δn which is injected through one contact and removed through the other. The transfer Δn follows from the relations $\mu_L(n + \Delta n)$ and $\mu_R(n - \Delta n)$ with n the filling of the system at zero voltage. Note that, the chemical potentials μ_L and μ_R must be chosen appropriately to ensure that the average filling is kept at n .

The net current obtained by applying a voltage is given by the average number of particles passing through the system per unit time after a steady state situation has been reached. Yet, the current not only depends on the particle transfer Δn as determined by the values of μ , μ_L and μ_R , but also on the strength of the coupling between battery and system. The latter is set by the properties of the battery contact and determines the rate at which transfers of magnitude Δn take place. The maximum current is obtained when subsequent transfers are separated by just the time it takes for one transfer of Δn to free up the site to which the battery is connected. This

is the regime we focus on because it yields the largest currents and reveals the limits on the currents which are due to the properties of the conductor material rather than due to the properties of the battery contact.

The steady state reached after a time of transient behavior takes the form of a running density wave whose amplitude is determined by the particle transfer Δn from the battery, hence by the voltage, and whose wavelength depends on the strength of the coupling between battery and wire. The maximum current is present when the wavelength is given by twice the lattice period. In that case, the maxima (minima) of the wave take the value $n + \Delta n$ ($n - \Delta n$). The steady state current is then essentially given by $I = 4\Delta n\nu$, with ν the frequency of the wave, since the time it takes to transport $2\Delta n$ particles through a single link is given by $\Delta t = 1/2\nu$. To give an example, in the simplest case of a single link in the absence of additional external potentials, it is given by $\Delta t = 1/2\nu$ where ν is the Rabi frequency $\nu = J/\hbar\pi$. In the limit of small voltages, the wave created by the contact with the battery can be described by the elementary excitations of the gas.

We estimate the steady state currents by considering systems which only have a few links. The idea underlying our calculation of the current response is that it mainly depends on the particle transfer Δn associated with a certain voltage and only negligibly on the number of lattice sites. Reducing the calculation down to only one or two links is possible since we are interested in the regime $J/U \ll 1$ where beyond next-neighbour correlations are of minor importance.

In the case of atomtronic wires and diodes we consider a single link because in these cases the steady state current is controlled by one type of link. While in a wire there is only one type of link, the current in a diode is controlled by transport through the link at the junction between P-type and N-type material. A two-link system needs to be considered to describe a transistor since in this case the current is controlled by both the links at the interfaces between base and collector and between base and emitter. Current in wires, in a diode and a transistor will be discussed in detail below.

In practice, we compute the dynamical evolution of the one- or two-link system we are interested in. The system is prepared in a non-stationary state corresponding to the configuration generated by the battery contact. The actual transfer of particles between system and battery is not part of the calculation. The role of the battery is taken into account in the choice of the initial state which involves an excess Δn on one side and a deficit Δn on the other. We determine the steady state current $2\Delta n/\Delta t$ where Δt is the time it takes for $2\Delta n$ particles to move from the initially higher populated site to its neighbour.

The lattices necessary to actually build atomtronic diodes and transistors must be large since their operation relies on the existence of superfluid and insulating phases, i.e. on the applicability of the phase diagram

Fig. 2. The importance of the phase diagram lies in determining the relation between chemical potential μ and filling n . As explained above, it is this relation which fixes the particle transfer Δn between battery terminal and atomtronic system at a certain voltage. Above all, it determines the range of voltages in which a change of voltage does not bring along a change in current because the battery chemical potentials lie in insulating zones where $\partial n / \partial \mu = 0$. Once we have obtained the data for the steady state current as a function of Δn , we use the large-system relation Eq. (2) for $\mu(n)$ to represent the current as a function of chemical potential difference, i.e. voltage.

III. ATOMTRONIC CONDUCTORS

The conductivity properties of the material change with the number of atoms in the lattice, i.e. with the lattice filling. The filling is increased as the chemical potential is raised. This moves the point in the phase diagram and yields either a superfluid or an insulating state (see Fig. 2). Changing the chemical potential is not the only way to control the filling and thus the properties of the material. In this section, we first discuss the possibility of varying the conductivity of a material by lattice doping. Secondly, we focus on the current-voltage characteristics of the different types of atomtronic materials.

A. Doped Materials

New materials with interesting properties can be designed by modifying the lattice potential in which the atoms are confined, and hence the band structure. This can be done in various ways. In the case of an optical lattice, the periodicity of the lattice can be modified by superimposing a periodic potential variation of different wavelength [36]. Disorder can be introduced by randomly modifying individual sites [37–39]. A further handle on the properties of the material is the symmetry of a 2D or 3D lattice [40–42]. Finally, it is conceivable to introduce a second atomic species, bosonic or fermionic, and to modify the properties of the material via inter-species interaction.

The atom analog of the doping of a semiconductor is particularly interesting. The aim of doping is to create energy levels in the energy gap between two bands. P-type doping is associated with energy levels located close to the upper edge of the highest full band while N-type doping gives rise to levels close to the lower edge of the first empty band. Both are accomplished by modifying the potential at individual lattice sites. N-type doping is achieved by replacing some lattice sites with donor sites. These correspond to potential wells which are slightly deeper than those of the unmodified lattice. Analogously, P-type doping requires introducing accep-

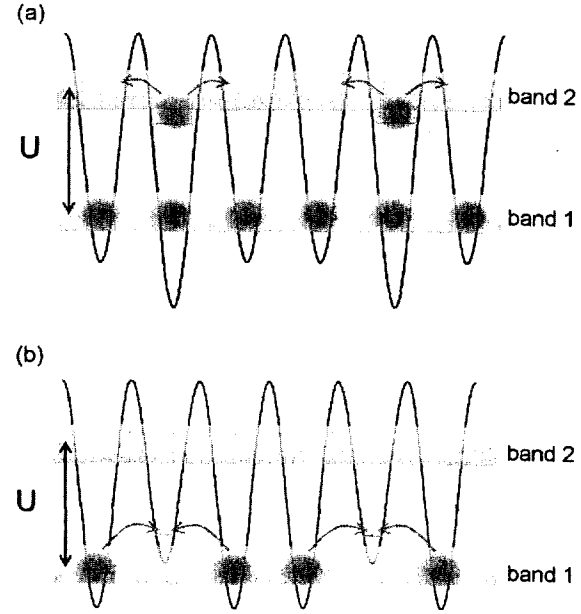


FIG. 4: (a) Schematics of an N-doped lattice. The donor sites feature a level right underneath the first empty band. An atom which occupies this level can easily be excited and move throughout the lattice.

(b) Schematics of a P-doped lattice. Acceptor sites have a level right above the highest full band. Atoms can easily be excited into this level and allow for a hole to move throughout the lattice.

tor sites of slightly shallower potential. The two potential configurations are shown in Fig. 4.

The advantage of doping is that it allows turning an insulator into a conductor without having to excite particles across the band gap into the empty conduction band. In atomtronics, this means that doping shifts the insulator zone in the phase diagram. Figure 5 compares the phase diagram of the undoped lattice with that of a P-doped and a N-doped lattice. N-type doping shifts the insulating zone downwards such that states that were previously in the insulating zone come to lie right above the insulating zone where the lattice has a full valence band and a few free carriers in the conduction band. Similarly, P-type doping shifts the insulating zone upwards such that states previously in the insulating region come to lie right below the insulating zone where the lattice has an almost full valence band with a few free hole carriers.

B. Material Current Properties

This section discusses the current response of atomtronic wires to an applied voltage. The magnitude of the current depends on the properties of the material and on the nature of the contact with the battery. The material can be in the Mott insulating phase or in the superfluid

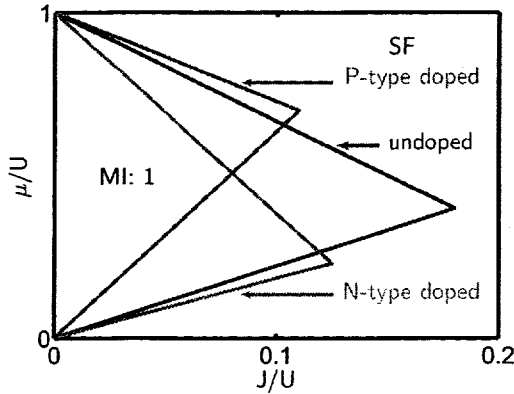


FIG. 5: Zero temperature phase diagram of a Bose gas in an undoped (blue), an N-doped (red) and a P-doped lattice (green). Displayed is the boundary of the lowest Mott insulator lobe with a filling of one atom per site as calculated using the two-state approximation. The results for the doped lattices were obtained by adding/subtracting an energy of $5J$ to/from every third site in a lattice with six sites. N-type doping turns an insulating state into a superfluid state with more than one atom per site. Similarly, P-type doping turns an insulating state into a superfluid state with less than one atom per site.

phase. In the Mott phase, a small voltage will not yield a current. Only at a large voltage, of the order of the gap U , will the battery be able to generate a current by feeding particles into the next unoccupied band. If the material is in the superfluid phase even a small voltage will suffice to generate a current. Due to the superfluid nature of the atomic carriers, this current is not slowed down by friction. Hence, the ratio of voltage to current does not have the physical meaning usually associated with resistance, but reflects the limits on the current at a given voltage due to factors other than decelerating friction. A primary limit is set by the hopping parameter J which quantifies how quickly atoms can move from one site to the next. Its value depends on the shape and the depth of the lattice. A further limit on the current is due to the interaction between the atoms. Their repulsion forces them to move in a highly correlated fashion. For this reason, the current does not grow linearly with the number of carriers at fixed voltage. Instead, the current per particle drops as more carriers are added and eventually goes to zero when the filling is one atom per site and the system becomes an insulator.

Apart from material dependent factors, it can be the nature of the contact with the battery which fixes the maximum achievable current. If it is more difficult for atoms to pass through the contact than to hop from one lattice site to the next then the current is not limited by J but by the rate at which the battery feeds in and removes particles. This situation is encountered when operating a battery in a regime of very weak coupling. The same

properties are present in electronic systems where there can be different types of contacts, such as rectifying and ohmic contacts [43]. Since we focus on the regime of maximum currents, currents are limited by the hopping parameter J and are not influenced by the properties of the battery contact.

As examples of the current-voltage characteristics of atomtronic wires, Fig. 6 presents the current as a function of voltage for lattices, or wires, of average filling $n = 1.1, 1.3, 1.5, 1.7, 1.9$. The curves for fillings with an equal number of free particles and holes coincide demonstrating the equivalence of hole and particle motion for $J/U \ll 1$. Since the gas is superfluid, the attainable currents are limited by the hopping parameter J and not by a dissipative mechanism that in electronic systems gives rise to a resistance. The maximum current attainable for a half-filled second band is $\sim 1.4 J/\hbar$. To give an example, note that in a cubic optical lattice with a depth of $10 E_R$ the hopping parameter $J \sim 0.02 E_R$, where $E_R = \hbar^2 \pi^2 / 2md^2$ is the recoil energy which is fixed by the lattice period d . For 87Rb and a lattice period of $d = 400\text{nm}$, the recoil energy is $E_R = (2\pi\hbar)3.55\text{kHz}$ yielding currents on the scale $J/\hbar \sim 2\pi 71\text{Hz}$ in a one-dimensional lattice.

The voltage in Fig. 6 is given in units of $\Delta\mu_{\text{max}}$. This quantity denotes the chemical potential differences that yields the maximum currents. It corresponds to the chemical potential difference at which the system, for a given filling, enters an insulating regime at one of the two battery contacts.

To better understand the current carrying characteristics of the different materials, the inset in Fig. 6 presents the currents at different average fillings, corresponding to different materials, at $\Delta\mu = \Delta\mu_{\text{max}}$. The plot is symmetric around its maximum at half filling reflecting particle-hole symmetry. Note that the average current per free particle, i.e. holes at $n > 1/2$, is constant. These current characteristics are very similar to those of semiconductor materials in that metals are good conductors while doped semiconductors do not conduct as well.

The data displayed in Fig. 6 is obtained from the dynamical evolution of a single link within the two-state approximation. The initial state is prepared with n_R and n_L particles on the right and left respectively. This is the state generated by applying a voltage $V = \mu_L - \mu_R$ with $\mu_L = \mu(n_L)$ and $\mu_R = \mu(n_R)$ where in general the relation between chemical potential and filling is obtained from the phase diagram and is given by Eq. (2) in the fermionized regime. The evolution of this initial state features the time-dependent current

$$i(t) = \frac{2J}{\hbar} (n_R - n_L) \sin(4Jt/\hbar) \quad (4)$$

from right to left. To obtain the steady state current we maximize the time average of Eq. 4 over a time interval Δt . This yields

$$I = 1.44 \frac{J}{\hbar} (n_R - n_L) \quad (5)$$

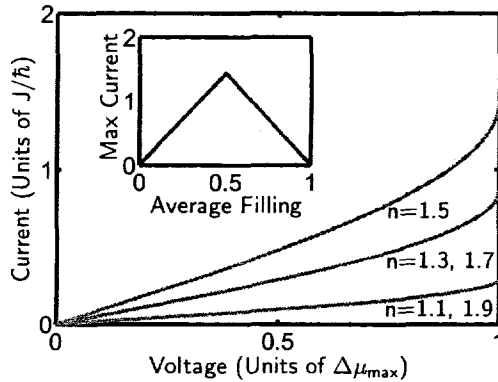


FIG. 6: Current as a function of chemical potential difference (voltage) for different materials (different fillings n) in the fermionization regime where bosons are impenetrable. A wire with a certain number of atoms carries the same current as a wire with that number of holes (particle-hole symmetry). The chemical potential difference is given in units of $\Delta\mu_{\max}$. This quantity denotes the chemical potential differences that yield the maximum currents and corresponds to the chemical potential difference at which the system enters an insulating regime at one of the two battery contacts for a given n . Inset: Current as a function of filling at $\Delta\mu_{\max}$. Maximum currents are attained at half filling. Note the symmetry in the current due to the particle-hole symmetry.

with $\Delta t = 0.83\hbar/J$. This value is close to the time it takes to invert the initial population imbalance, i.e. to complete half a cycle of frequency $\nu = 2J/\pi\hbar$. Note that the initial state is chosen to be the state with the lowest possible energy given the filling n and the population difference $n_R - n_L$. From the results for $I(\Delta\mu)$ we obtain the current-voltage dependence $I(\Delta\mu)$ via Eq. (2).

IV. ATOMTRONIC DIODES

A diode is a circuit element which features a highly asymmetric current-voltage curve. It allows a large current to pass in one direction, but not in the other. Thus, the analog of a diode is an atomtronic circuit element that lets an atomic current pass through when applying a voltage $V = \mu_L - \mu_R$ while $V = -(\mu_L - \mu_R)$ does not generate a current or only a small saturation current.

In solid state electronics, diodes are built by setting up a PN-junction in which a P-type semiconductor is brought into contact with an N-type semiconductor. Electrons move through the junction until an equilibrium is reached. This process depletes the junction region of free charges, leaving behind the static charges of the donor and acceptor impurities. As illustrated in Fig. 7(a), this creates an effective potential step across the junction. When a reverse bias voltage is applied the energy barrier is increased reducing the flux of electrons

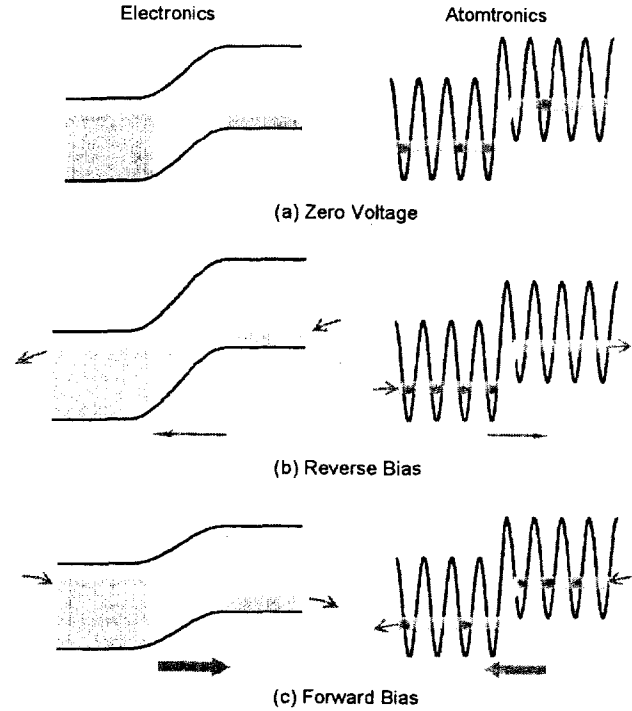


FIG. 7: Schematic of the conduction band of an electronic (left panels) and atomtronic (right panels) PN-junction diode in (a) equilibrium, (b) reverse bias and (c) forward bias with N-type materials on the left and P-type on the right of each configuration.

Left panels: The electronic system features a voltage dependent energy barrier at the junction leading to an increasing (decreasing) flux from the N-type to the P-type material as the junction is forward (reverse) biased while the current from P to N is independent of voltage.

Right panels: The operation of an atomtronic diode is based on the existence of insulating phases where $\partial n/\partial\mu = 0$, i.e. a change in voltage does not lead to a change in particle transfer between battery and system. As a consequence, only a small current can flow from N-component to P-component through an atomtronic diode in reverse bias while in forward bias the particle transfer between battery and system can be varied over a large range.

from N to P. At the same time the number of electrons that can fall down the step remains constant giving rise to a reverse bias saturation current that is independent of voltage (see Fig. 7 (b)). However, if the diode is forward biased, more electrons are able to move from the N-type to the P-type material than at equilibrium since the potential barrier is decreased by the forward bias voltage (see Fig. 7(c)). A detailed discussion of the diode behavior of a semiconductor PN-junction can for example be found in [43].

A. Diode PN-junction configuration

As discussed previously, we can design atomtronic wires whose conductivity properties can be described by locating the material's chemical potential in its phase diagram. The properties of the material can be changed by either changing its chemical potential or by modifying the lattice and thereby altering the phase diagram. As particular examples, we have discussed the analog of P- and N-type doped conductors.

Materials which are composed of several types of atomtronic conductors can be produced by connecting lattices of different doping. Another possibility to build a junction is to superimpose additional external potentials, for example a simple potential step. This has the effect of shifting the phase diagram of a part of the lattice upwards or downwards with respect to that of the rest. Sufficiently far away from the junction, the state of the different components can be accurately described by the phase diagrams of the individual materials. In fact, we have found that the boundary only affects one to two sites of each component in the limit $J/U \ll 1$. This means that a local chemical potential can be associated with each component of the conductor which can be located in each material's phase diagram. Thereby, the local conductivity properties can be identified. Of course, at equilibrium, i.e. at zero voltage, the composite material is actually described by a single chemical potential μ but it is μ relative to the zero point energy of each lattice site that determines the filling of each site.

The conduction band of a semiconductor PN-junction features a small thermal electron population on the P-side and a considerably larger electron filling on the N-side. The atomtronic analog can be obtained by bringing into contact P-type and N-type lattices. Alternatively, it can be attained by imposing an external potential step. In the following, we focus on this latter implementation. The main characteristics of the diode behavior are not affected by this choice. An example for a possible equilibrium configuration is represented by the squares in Fig. 8. The potential step could be generated experimentally by exposing one part of the system to off-resonant laser light.

B. Diode current-voltage characteristics

To achieve diode characteristics, we exploit the possibility of undergoing a quantum phase transition to the insulating phase. The materials are configured such that the chemical potentials of the battery poles remain in the superfluid regime when hooking up the battery in one direction, but they easily enter insulating regimes when the voltage is applied in the opposite direction.

The effect of applying a voltage is illustrated in Fig. 8. Forward bias is achieved by connecting the P-side to the low voltage pole and the N-side to the high voltage pole of the battery. In this situation, the chemical potentials of the battery poles are located in the superfluid region

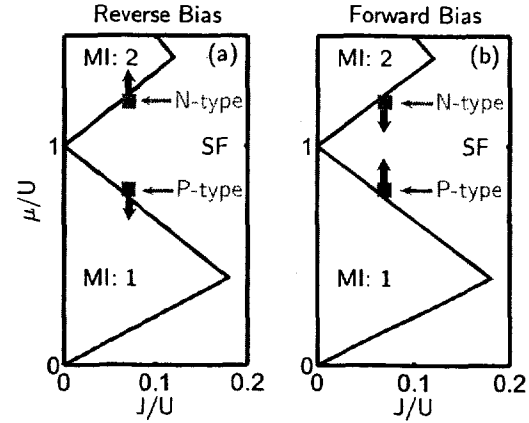


FIG. 8: Phase diagram of the PN-junction configuration of an atomtronic diode. The small population of the second band in the P-material yields the analog of the small thermal electron population of the conduction band in a semiconductor. The states of the P-type and N-type materials at zero voltage are represented by the squares. Arrows indicate the chemical potential difference (voltage) imposed to obtain a reverse (left) and a forward biased junction (right).

of the phase diagram and atoms can flow from the P-component to the N-component. The larger the applied voltage, the larger the generated current. When the battery contacts are switched, the diode is reverse biased. As the voltage is increased a small current starts flowing. However, as soon as the voltage is large enough to make the battery chemical potentials enter the insulating zones, the current can not increase any further. As a consequence, the current-voltage curve is asymmetric. The remnant current obtained in reverse bias, the saturation current, becomes smaller as the components' initial states are moved closer to the insulating phase.

Figure 7 presents a schematic comparison of the conduction band of an electronic and an atomtronic diode obtained using a step potential. For the atomtronic diode, the fact that only a small current can flow in reverse bias is not due to the presence of a voltage-dependent energy barrier at the junction as in the electronic case. Instead, it arises from the battery chemical potentials moving into insulating zones corresponding to a full conduction band on the N-side and an empty conduction band on the P-side. An important difference between electronic and atomtronic case is the opposite direction of current flow. In forward bias, atoms flow from the P-type to the N-type material rather than the other way around as electrons in a semiconductor.

Figure 9 displays the highly asymmetric current-voltage curve obtained from our calculation. The potential step is chosen such as to yield an equilibrium configuration with a filling of 1.99 and 1.01 atoms on the N-side and P-side respectively. In this configuration, we obtain a saturation current of $0.14 J/\hbar$ while in forward bias, currents can exceed $1.4 J/\hbar$. Note that the current changes strongly in the vicinity of $V = 0$. This

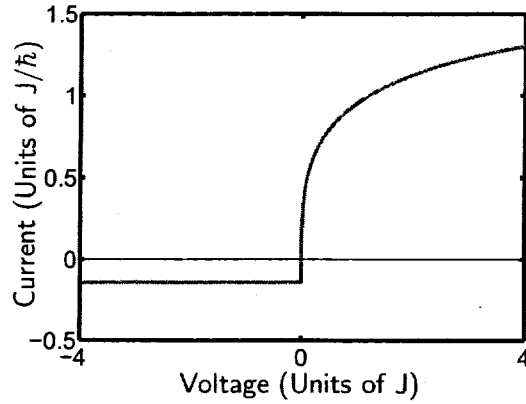


FIG. 9: The characteristic current-voltage curve for an atomtronic diode. The larger the forward bias (voltage > 0), the higher the current of atoms flowing from the P-component and to the N-component. In reverse bias (voltage < 0) the current saturates since the particle transfer between battery and system can not be increased beyond a certain small value when the battery pole chemical potentials enter insulating zones where $\partial n_i / \partial \mu = 0$.

is reminiscent of the behavior of an electronic diode as the temperature approaches zero. Reducing the potential step lowers the population difference between P- and N-component at equilibrium and leads to an increase in saturation current and to a decrease of the slope of the current-voltage curve around $V = 0$.

The diode currents have been calculated analytically in the same manner as the currents carried by atomtronic wires (see section III B above) except for the addition of the potential energy step between the two sites. From the result for the relation $I(\Delta n)$ we obtain the current-voltage dependence $I(\Delta \mu)$ using Eq. (2).

V. ATOMTRONIC TRANSISTOR

As in electronics, the highly asymmetric current-voltage curve of atomtronic diodes can be exploited to build a transistor. Bipolar junction transistors (BJT) are circuit elements can serve as amplifiers or switches. In electronics, they consist either of a thin P-type layer sandwiched between two N-type components (NPN) or a thin N-type layer between two P-type components (PNP). For our discussion, we consider an NPN transistor. A detailed discussion of semiconductor bipolar junction transistors can, for example, be found in [43]. The basic circuit schematic is displayed in Fig. 10. The voltage V_{BC} which is applied to the PN-junction formed by the middle component, the base, and one of the outer components, the collector, puts this junction into reverse bias. At the same time, the other junction formed by the base and the other outer component, the emitter, is put into forward bias by applying a voltage V_{EB} . The

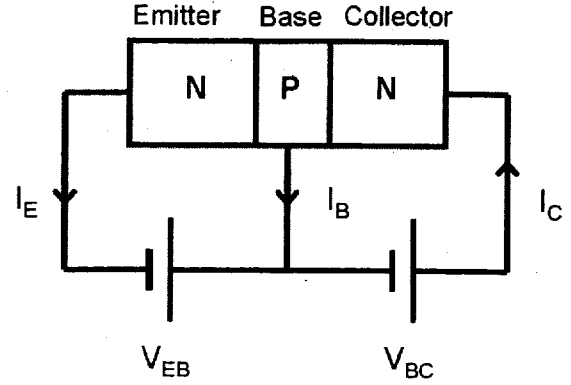


FIG. 10: Circuit schematic of an electronic or atomtronic bipolar junction transistor of the NPN-type. A thin P-type component (base) is sandwiched between two N-type components (emitter and collector). The key feature is that the voltage V_{EB} can be used to obtain gain in the collector current I_C relative to the base current I_B .

key idea is to use the voltage V_{EB} to control the current I_C leaving the collector element and thereby achieve gain in I_C relative to the base current I_B . At $V_{EB} = 0$ one is simply dealing with the reverse biased base-collector junction. In this case, the currents I_C and I_B both equal the small reverse bias saturation current of the base-collector junction. The collector current I_C grows drastically when V_{EB} is increased such that the emitter-base junction is forward biased. This effect relies on the base region being very thin. The forward bias gives rise to a flow of electrons from the emitter into the base region, thereby significantly increasing the number of electrons at the base-collector junction. Recall that at $V_{EB} = 0$, the base is depleted of electrons by the reverse bias V_{BC} . The emitter-base junction thus serves to greatly modify the number of carriers in the base which are subjected to the base-collector reverse bias. This leads to an increase of I_C beyond the saturation current. Since the base is extremely thin there is less opportunity for the electrons to leave the base compared to entering the collector. Because of this, most of the current that enters the base from the emitter moves on to the collector instead of it leaving out the base terminal. Therefore the relative changes in the current from the base I_B and from the collector I_C yields a large differential gain dI_C/dI_B .

These key features of an electronic transistor can be translated into atomtronics with atoms taking the place of electrons. The important point is to mimic the carrier densities and thus the filling of the three components, emitter, base and collector. This can be achieved by doping or, equivalently, by using potential steps. As for the diode case, we focus on the latter implementation. The atomtronic transistor can be created by setting up a configuration such that for zero voltage the left and right regions have a large filling compared to the sandwiched thin

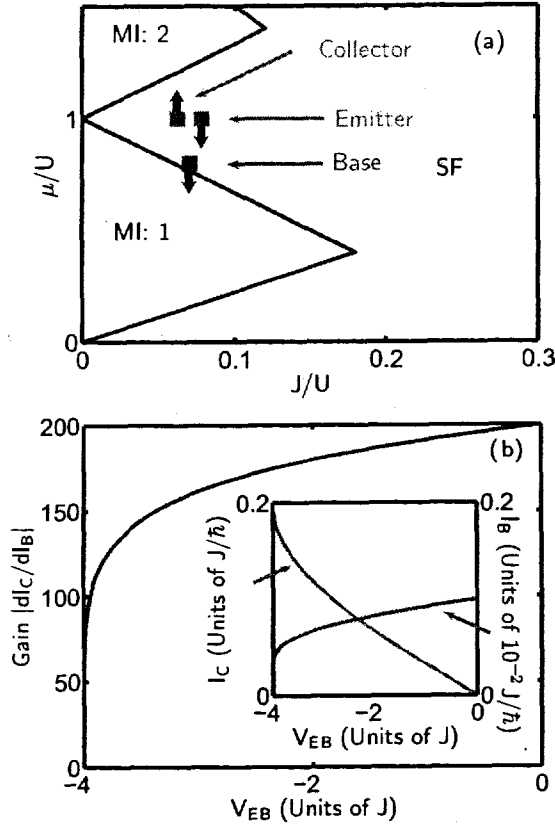


FIG. 11: (a) Squares: The equilibrium configuration of an atomtronic bipolar junction transistor in the phase diagram. Arrows: Direction in which the chemical potentials of the battery contacts are varied.

(b) Differential gain dI_C/dI_B as a function of emitter-base voltage V_{EB} .

Inset: Base current and collector current as a function of emitter base voltage. The voltage is changed by varying the emitter contact potential from $\mu(n_E = 1)$ to $\mu(n_E = 1.5)$. The base contact is kept at $\mu(n_B = 1)$ right below its equilibrium value $\mu(n_B = 1.005)$ while the collector contact is kept at the equilibrium value $\mu(n_C = 1.5)$.

base region. The phase diagram for such an arrangement is depicted in Fig. 11(a), where the squares represent the equilibrium configuration, while the arrows indicate the way the battery chemical potentials are tuned. A small voltage is applied to the collector-base junction such that a small current flows from the collector into the base. When the emitter battery contact chemical potential μ_E is lowered, atoms move from base to emitter and leave through the emitter, giving rise to a non-zero emitter current I_E . As a back-effect, this leads to an increase in I_C since the fast removal of atoms from the base through the emitter allows more atoms to move into the base from the collector.

Meanwhile, the base current I_B becomes smaller the

further the emitter chemical potential μ_E is lowered. This is due to the base being very thin relative to the emitter and the collector, so atoms traverse preferentially from collector to emitter rather than leaving out the base contributing to I_B . The effect of the forward bias V_{EB} on the base current I_B is thus opposite to its effect on I_C . Therefore, our atomtronic transistor features an inverted amplification in which a small decrease in the base current goes along with a large increase in the collector current (negative gain).

An example for the behavior of the currents in an atomtronic transistor is given in Fig. 11(b). The equilibrium configuration has 1.5 atoms per site in emitter and collector and 1.005 atoms per site in the base. In Fig. 11(b) we plot data obtained for the individual currents I_C , and I_B upon variation of the emitter chemical potential μ_E while keeping the base battery contact at a chemical potential $\mu(n_B = 1)$ in the $n = 1$ Mott-insulating zone. To demonstrate differential gain we display the quantity $|dI_C/dI_B|$ as a function of V_{EB} .

The data presented in Fig. 11(b) is obtained from the dynamics of a three-well lattice. An external potential is added which raises the middle site. This site plays the role of the base while the outer sites represent emitter and collector. The initial state is prepared as the lowest energy solution with n_E atoms in the emitter and $n_C = 1.5$ atoms in the collector. The current of atoms passing through the base from collector to emitter is given by $i_C = (i_{CB} + i_{BE})/2$ with i_{CB} the current from collector to base and i_{BE} the current from base to emitter. As in the previous sections, we calculate the steady state current I_C by maximizing the time average of i_C . From the result for the relation $I_C(\Delta\mu)$ we obtain the current-voltage dependence $I(\Delta\mu)$ using Eq. (2).

Since we are interested in μ_E -dependence of I_C at fixed V_{BC} the initial collector occupation is kept fixed at $n_C = 1.5$ while the emitter occupation n_E is varied in the range $1 \leq n_E < 1.5$. The base current is set to be $I_B = \Gamma n_B$, where Γ must satisfy the condition $\Gamma \ll J/\hbar$. The quantity Γ describes the weak coupling with the battery at the base contact which is due to the thinness of the base. The data for I_B displayed in Fig. 11(b) is obtained using $\Gamma = 0.01J/\hbar$. Note that our calculation neglects the effect of I_B on I_C . This is justified because the weak coupling at the base contact implies that the reduction of n_B by I_B is small. Note that, overall, the possibility for transistor current gain relies on two factors. The base region must be thin and the emitter must have an equilibrium filling significantly larger than the base.

VI. REMARKS

We have showed how strongly interacting ultracold bosonic gases in periodic potentials can be used as conductors in a circuit and how they can be used to build atom analogs of diodes and bipolar junction transistors.

From here, the implementation of an atom amplifier is immediate. An atom amplifier is a device which allows control of a big atomic current with a small one. The transistor presented above directly serves this purpose since small changes in the base current bring along large changes in the collector current. From here, it is straight forward to conceive of more complex devices such as a flip flop, a bistable device that uses cross negative feedback between two transistors.

The similarity in qualitative behavior goes along with a number of significant differences in the underlying physics. Firstly, in the atom case the band gap results from interactions rather than from statistics as in electronics. Secondly, the atomic currents are superfluid. As a consequence, the ratio between voltage and current has the meaning of a dissipationless resistance. Further differences arise in both diodes and transistors. Our atomtronic diode does not feature a depletion layer, i.e. it does not exhibit a voltage-dependent energy barrier at the junction. The asymmetry in the current-voltage curve results from voltage-sign dependent transitions to an insulating phase. As a consequence, atoms flow from P to N in forward bias rather than flowing, as in electronics, from N to P. Note that this difference can not be resolved by drawing the analogy between atom holes and electrons rather than atoms and electrons since this would also require relabeling the N-type material as P-type and vice versa and hence the current direction would again be reversed in comparison to the electronic case. Due to the difference in diode behavior the atomic collector current in a transistor flows from collector into base and the emitter current flows from base into emitter, i.e. opposite to electronic flow in a NPN transistor. A significant difference in the qualitative behavior of electronic and atomtronic transistor is given by the gain being negative in the atomtronic case. The collector current increases as base current decreases. We expect that this does not affect the functionality of devices based on the operation of

bipolar junction transistors. Yet, an adaptation of their design will be necessary.

The data presented in this paper is obtained from calculations for a one-dimensional lattice. This choice is of an entirely practical nature. The basic ideas also hold for two- and three-dimensional cubic lattices and extend to other lattice geometries which make transitions between superfluid and insulating phases upon changes of the chemical potential.

An issue to be addressed in the future is that of the noise associated with the inherent quantum uncertainty of the current carrying states given the context of the coherent transport of atoms.

Finally, it is important to keep in mind that this paper develops atomtronics within the Bose-Hubbard model. This model provides an excellent description of ongoing experiments with ultracold bosonic atoms in optical lattices. Other Hamiltonians might offer alternative ways of drawing the analogy with electronics. A natural choice for further study are Hamiltonians describing bosons with beyond onsite interactions and Hamiltonians for fermionic gases.

VII. ACKNOWLEDGEMENTS

We thank John Cooper, Rajiv Bhat and Brandon M. Peden for useful discussions. This work was supported by the Defense Advanced Research Projects Agency's Defense Science Office through a PINS program (Grant No. W911NF-04-1-0043) and the Air Force Office of Scientific Research (Grant No. FA9550-04-1-0460). We also acknowledge support of the Department of Energy, Office of Basic Energy Sciences via the Chemical Sciences, Geosciences, and Biosciences Division, furthermore of the National Science Foundation (B. T. S.) and the Deutsche Forschungsgemeinschaft (M. K.).

-
- [1] B. P. Anderson and M. A. Kasevich, *Science* **282**, 1686 (1998).
 - [2] F. Cataliotti, S. Burger, C. Fort, P. Maddaloni, F. Minardi, A. Trombettoni, A. Smerzi, and M. Inguscio, *Science* **293**, 843 (2001).
 - [3] M. Greiner, I. Bloch, O. Mandel, T. W. Hänsch, and T. Esslinger, *Phys. Rev. Lett.* **87**, 160405 (2001).
 - [4] O. Morsch, J. Müller, M. Cristiani, D. Ciampini, and E. Arimondo, *Phys. Rev. Lett.* **87**, 140402 (2001).
 - [5] J. Denschlag, J. Simsarian, H. Häffner, C. McKenzie, A. Browaeys, D. Cho, K. Helmerson, S. Rolston, and W. Phillips, *J. Phys. B: At. Mol. Opt. Phys.* **35**, 3095 (2002).
 - [6] G. Modugno, F. Ferlaino, R. Heidemann, G. Roati, and M. Inguscio, *Phys. Rev. A* **68**, 011601 (2003).
 - [7] G. Roati, E. de Mirandes, F. Ferlaino, H. Ott, G. Modugno, and M. Inguscio, *Phys. Rev. Lett.* **92**, 230402 (2004).
 - [8] L. Pezze, L. Pitaevskii, A. Smerzi, S. Stringari, G. Modugno, E. de Mirandes, F. Ferlaino, H. Ott, G. Roati, and M. Inguscio, *Phys. Rev. Lett.* **93**, 120401 (2004).
 - [9] C. Fort, F. Cataliotti, J. Catani, L. De Sarlo, L. Fallani, J. Lye, M. Modugno, R. Saers, and M. Inguscio, *Laser Physics* **15**, 447 (2005).
 - [10] M. Köhl, H. Moritz, T. Stöferle, K. Günter, and T. Esslinger, *Phys. Rev. Lett.* **94**, 080403 (2005).
 - [11] M. Greiner, O. Mandel, T. Esslinger, T. W. Hänsch, and I. Bloch, *Nature (London)* **415**, 39 (2002).
 - [12] T. Stöferle, H. Moritz, C. Schori, M. Köhl, and T. Esslinger, *Phys. Rev. Lett.* **92**, 130403 (2004).
 - [13] A. Ruschhaupt and J. G. Muga, *Phys. Rev. A* **70**, 061604 (2004).
 - [14] A. Micheli, A. J. Daley, D. Jaksch, and P. Zoller, *Phys. Rev. Lett.* **93**, 140408 (2004).
 - [15] A. Ruschhaupt, F. Delgado, and J. G. Muga, *J. Phys. B: At. Mol. Opt. Phys.* **38**, 2665 (2005).
 - [16] A. Ruschhaupt and J. G. Muga, *Phys. Rev. A* **73**, 013608 (2006).

- (2006).
- [17] A. Ruschhaupt, J. G. Muga, and M. G. Raizen, *J. Phys. B: At. Mol. Opt. Phys.* **39**, L133 (2006).
 - [18] A. Daley, S. Clark, D. Jaksch, and P. Zoller, *Phys. Rev. A* **72**, 043618 (2005).
 - [19] A. Micheli and P. Zoller, *Phys. Rev. A* **73**, 043613 (2006).
 - [20] J. Stickney, D. Z. Anderson, and A. Zozulya, to be published.
 - [21] S. Rolston and W. Phillips, *Nature (London)* **416**, 219 (2002).
 - [22] K. Bongs and K. Sengstock, *Rep. Prog. Phys.* **67**, 907 (2004).
 - [23] C. Search and P. Meystre, in *Progress in Optics*, ed. E. Wolf (Elsevier, Amsterdam, 2005), Vol. 47.
 - [24] G. Brennen, C. Caves, F. Jessen, and I. Deutsch, *Phys. Rev. Lett.* **82**, 1060 (1999).
 - [25] H. Briegel, T. Calarco, D. Jaksch, J. Cirac, and P. Zoller, *J. Mod. Opt.* **47**, 415 (2000).
 - [26] A. Steane, *Rep. Prog. Phys.* **61**, 117 (1998).
 - [27] R. Folman, P. Krüger, J. Schmiedmayer, J. Denschlag, and C. Henkel, *Adv. At. Mol. Opt. Phys.* **48**, 263 (2002).
 - [28] J. Reichel, *Appl. Phys. B* **75**, 469 (2002).
 - [29] W. Zwerger, *J. Opt. B* **5**, S9 (2003).
 - [30] M. P. A. Fisher, P. B. Weichman, G. Grinstein, and D. S. Fisher, *Phys. Rev. B* **40**, 546 (1989).
 - [31] P. Jordan and E. Wigner, *Z. Phys.* **47**, 631 (1928).
 - [32] S. Sachdev, *Quantum Phase Transitions* (Cambridge Univ. Press, Cambridge, 1999).
 - [33] R. Bhat, M. J. Holland, and L. D. Carr, *Phys. Rev. Lett.* **96**, 060405 (2006).
 - [34] The lower/upper boundary of the m th Mott zone is obtained by applying the two-state approximation to the m th/ $(m + 1)$ th band, where $m = 1, 2, \dots$ is the band index. The tip of the zone, given by the intersection of the two boundaries, yields a good estimate of the value of J/U at which the superfluid-insulator transition occurs at integer filling.
 - [35] B. M. Peden, to be published.
 - [36] S. Peil, J. V. Porto, B. L. Tolra, J. M. Obrecht, B. E. King, M. Subbotin, S. L. Rolston, and W. D. Phillips, *Phys. Rev. A* **67**, 051603 (2003).
 - [37] P. Horak, J.-Y. Courtois, and G. Grynberg, *Phys. Rev. A* **58**, 3953 (1998).
 - [38] H. Gimperlein, S. Wessel, J. Schmiedmayer, and L. Santos, *Phys. Rev. Lett.* **95**, 170401 (2005).
 - [39] T. Schulte, S. Drenkelforth, J. Kruse, W. Ertmer, J. Arlt, K. Sacha, J. Zakrzewski, and M. Lewenstein, *Phys. Rev. Lett.* **95**, 170411 (2005).
 - [40] L. Santos, M. Baranov, J. Cirac, H. Everts, H. Fehrmann, and M. Lewenstein, *Phys. Rev. Lett.* **93**, 030601 (2004).
 - [41] L. Sanchez-Palencia and L. Santos, *Phys. Rev. A* **72**, 053607 (2005).
 - [42] G. Grynberg and C. Robilliard, *Phys. Rep.* **355**, 335 (2001).
 - [43] P. D. Ankrum, *Semiconductor Electronics* (Prentice-Hall, Englewood-Cliffs, N.J., 1971).